

# Wavelet Domain Residual Network (WavResNet) for Low-Dose X-ray CT Reconstruction

Eunhee Kang  
KAIST  
Daejeon, Korea  
Email: keh0220@kaist.ac.kr

Junhong Min<sup>†</sup>  
Samsung Electronics Co.  
Suwon, Korea  
Email: gminimok@gmail.com

Jong Chul Ye\*  
KAIST  
Daejeon, Korea  
Email: jong.ye@kaist.ac.kr

**Abstract**—Model based iterative reconstruction (MBIR) algorithms for low-dose X-ray CT are computationally complex because of the repeated use of the forward and backward projection. Inspired by this success of deep learning in computer vision applications, we recently proposed a deep convolutional neural network (CNN) for low-dose X-ray CT and won the second place in 2016 AAPM Low-Dose CT Grand Challenge. However, some of the texture are not fully recovered, which was unfamiliar to the radiologists. To cope with this problem, here we propose a direct residual learning approach on directional wavelet domain to solve this problem and to improve the performance against previous work. In particular, the new network estimates the noise of each input wavelet transform, and then the de-noised wavelet coefficients are obtained by subtracting the noise from the input wavelet transform bands. The experimental results confirm that the proposed network has significantly improved performance, preserving the detail texture of the original images.

## I. INTRODUCTION

Due to the risk of radiation exposure, methods for minimizing X-ray dose have been extensively studied. A reduction in the number of X-ray photons emitted can solve the problem of radiation exposure. However, it brings the low signal-to-ratio (SNR) measurements that cause the noise in the reconstruction results. The noise of low-dose CT is usually approximated by Gaussian model, but CT specific streaking noise is also included in the low-dose CT images. Streaking noise occurs due to the photon starvation and beam hardening from sophisticated non-linear X-ray photon acquisition processes. To cope with these problems, model based iterative reconstruction (MBIR) algorithms have been investigated [1], [2]. However, MBIR have the limitations because of computationally extensive iterative applications of forward and backward projection.

Nowadays, extensive data is available, so it is desirable to use this database. In the computer vision community, deep convolution neural network (CNN) were actively investigated using the large data and high-performance graphical processing units (GPUs) [3]. With the developments of new network units such as rectified linear unit (ReLU), max pooling and batch normalization, the classical training problems are solved and the networks are given deep structures. Deep network has achieved the great performance improvement in low-level computer vision applications such as denoising [4] and super-resolution [5].

In the area of medical imaging, there are also extensive research activities that use deep learning. However, most of these

studies focus on image-based diagnostics, and its applications for image reconstruction problems such as x-ray computed tomography (CT) reconstruction are relatively less studied. Recently, we have introduced a wavelet domain deep learning algorithm for low-dose X-ray CT algorithm [6], whose validity has been rigorously confirmed by winning the second place award in AAPM Low-Dose CT Grand Challenges. However, in this earlier work, the reconstruction results lost some texture of the original images. Therefore, one of the most important contributions of this paper is the development of a drastically improved deep network, which overcomes the limitations of previous work by maintaining detailed textures and edges to improve the performance.

The key to such an improvement is the observation that the low-dose noise artifacts in wavelet domain has a much simpler topology than the original full-dose images so that the learning of the artifact signal is easier than learning the full-dose images. Once the noise in the wavelet domain is estimated, the denoised wavelet coefficients are obtained by subtracting the estimated noise from the wavelet coefficients of input low-dose X-ray CT images. Then, the final image is obtained by executing wavelet recomposition. Because the learning is done to estimate the wavelet domain residual signals, we call the new deep learning algorithm as *wavelet domain residual network (WavResNet)*.

## II. THEORY

### A. Deep learning in higher dimensional feature space

In a learning problem, based on a observation (*input*)  $X \in \mathcal{X}$  and a *label*  $Y \in \mathcal{Y}$  generated by a distribution  $D$ , we are interested in estimating a regression function  $f : X \rightarrow Y$  in a functional space  $\mathcal{F}$  that minimizes the risk  $L(f) = E_D \|Y - f(X)\|^2$ . However, an important technical issue is that the associated probability distribution  $D$  is unknown. Moreover, we only have a finite sequence of training data set  $S = \{(X_1, Y_1), \dots, (X_n, Y_n)\}$ , so there is only an empirical risk  $\hat{L}_n(f) = \frac{1}{n} \sum_{i=1}^n \|Y_i - f(X_i)\|^2$ . A direct minimization of empirical risk is, however, problematic because of the overfitting.

To solve this problem, statistical learning theory [7] has been developed to bound the risk of a learning algorithm in terms of complexity (eg. VC dimension, shatter coefficients, etc) and the empirical risk. Rademacher complexity [8] is

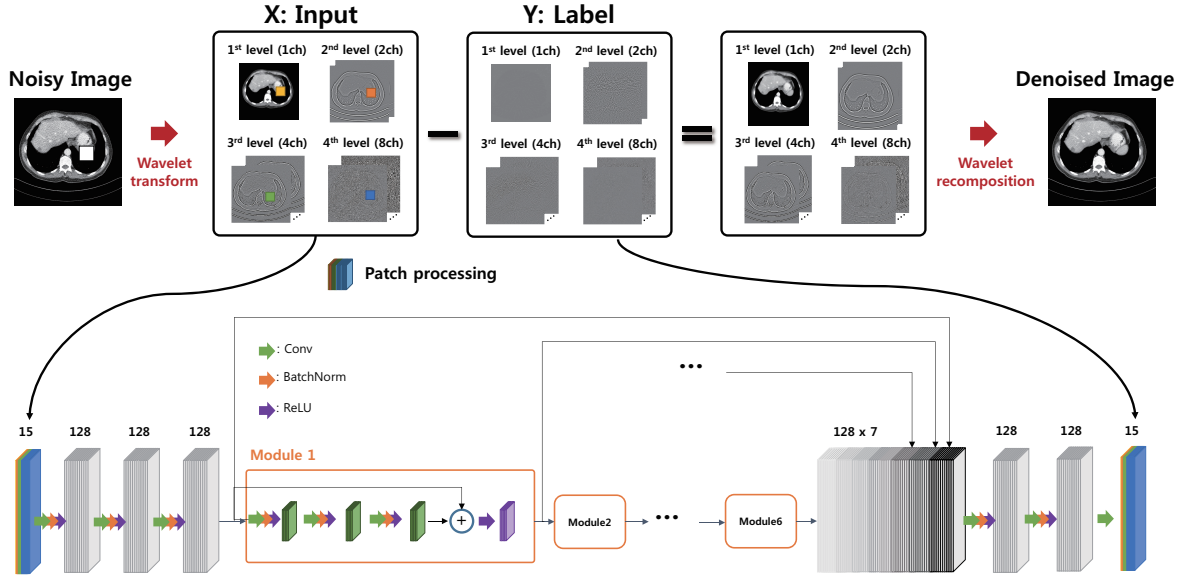


Fig. 1. The proposed WavResNet architecture for low-dose X-ray CT reconstruction.

one of the most modern notions of complexity, which is distribution-dependent and defined for any class of real-valued functions. Specifically, with probability  $\geq 1 - \delta$ , for every function  $f \in \mathcal{F}$ ,

$$L(f) \leq \underbrace{\hat{L}_n(f)}_{\text{empirical risk}} + \underbrace{2\hat{R}_n(\mathcal{F})}_{\text{complexity penalty}} + 3\sqrt{\frac{\ln(2/\delta)}{n}} \quad (1)$$

where the empirical Rademacher complexity  $\hat{R}_n(\mathcal{F})$  is defined to be

$$\hat{R}_n(\mathcal{F}) = E_\sigma \left[ \sup_{f \in \mathcal{F}} \left( \frac{1}{n} \sum_{i=1}^n \sigma_i f(X_i) \right) \right],$$

where  $\sigma_1, \dots, \sigma_n$  are independent random variables that are uniformly chosen from  $\{-1, 1\}$ .

Here, empirical risk is determined by the representation power of the network [9], while the complexity is determined by the structure of a network. The capacity of functions grows exponentially with respect to the number of hidden units [9]. When the network architecture is determined, its capacity is fixed. Therefore, the performance of the network is now dependent on the complexity of the label  $Y$  that a given deep network tries to approximate.

One of the most important contributions of this paper is to extend this idea to a novel deep network design principle. Specifically, for a given deep network  $f : X \rightarrow Y$ , our design goal is to find  $T$  and  $S$  maps that embed the input and label data sets to high dimensional features space. Thus, the resulting data sets  $X' = T(X)$  and  $Y' = S(Y)$  may have simpler data manifold. This can be shown in the following

diagram:

$$\begin{array}{ccc} X & \xrightarrow{g} & Y \\ T \uparrow & & \downarrow S \\ X' & \xrightarrow{f} & Y' \\ & & \uparrow S^\dagger \\ & & T^\dagger \end{array}$$

where the superscript  $\dagger$  denotes the pseudo-inverse that restore the original input data from high-dimensional features. Then, it is our goal to find a neural network  $f : X' \rightarrow Y'$  in the feature space that is executed better than in the original image space. Note that this idea resembles the *kernel trick* [10] in support vector machines, which designs a linear classifier in high dimensional feature space using nonlinear kernels.

We are aware that the basic motivation of deep learning is to automatically extract the embedding of the feature space by learning; thus, additional embedding by  $T$  and  $S$  appear redundant. Although true in theory, in many of the medical image reconstruction problems, the database is usually not large enough. Thus, analytic form of the embedding at the input and output ends provides many practical advantages and improved performance. For example, in recent deep residual learning [11], the input transform  $T$  is an identity mapping and the label transform is given by

$$Y' = S(Y) = Y - X \quad ,$$

which we call a *residual transform*. In other word, the output embedding is to provide the residual between the artifact-free output and noisy input so that the learning is performed to learn the residual. Using persistent homology analysis, our recent work [12] showed that the label manifold of the residual data is topologically simpler than that of  $Y$ .

## B. Proposed embedding scheme

Inspired by this finding, this paper proposes a high dimensional embedding scheme to directional wavelet transform domain residual signals. More specifically, the wavelet transform can annihilate the smoothly varying signals while maintaining the image edges due to the vanishing moments of wavelets, resulting in the dimensional reduction and manifold simplification. Furthermore, low-dose X-ray CT images exhibits streaking noise. Therefore, directional wavelet transform, such as contourlet transform, has directional filter banks that are good in detecting the streaking noise patterns and the directional edge information of X-ray CT images. In addition, the contourlet transform is a redundant transform, so the associated embedding to higher dimensional features space is good for learning. Therefore, by combining these with the observation that the residual signals have a simpler topological structures, our proposed embedding  $T$  for the input space is contourlet transform and the  $S$  for the label is the residual transform in the contourlet domain, i.e.

$$\begin{aligned} X' = T(X) &= \text{Contourlet Transform}(X) \\ Y' = S(Y) &= T(Y) - T(X). \end{aligned}$$

The resulting WavResNet structure is illustrated in Fig. 1.

## III. METHOD

### A. Network architecture

In detail, the non-subsampled contourlet transform consists of two steps [13]; non-decimated multi-scale decomposition and directional decomposition. as shown in upper part of the Fig. 1. The filter bank does not have down-sampling or up-sampling, so it is shift invariant. We used the four level decomposition resulting in 15 bands.

The proposed deep network is shown in lower part of the Fig. 1. It contains 24 convolution layers, followed by a batch normalization layer and a ReLU layer except the last convolution layer. At the first convolution layer, 128 set of  $3 \times 3 \times 15$  convolution kernels are used. Then, 128 set of  $3 \times 3 \times 128$  convolution kernels are used in the following convolution layers. The module has 3 sets of convolution, batch normalization, and ReLU layers, and 1 bypass connection has a ReLU layer. Out deep network consists of 6 modules and has a channel concatenation layer that stacks several inputs of the individual modules. This allows gradients to be back-propagated over different paths.

### B. Network training

We trained the proposed deep network by the conventional error back-propagation with stochastic gradient descent (SGD) scheme. The learning rate was initially set to 0.01 and decreased continuously down to  $10^{-5}$ . We used the gradient clipping method in the range  $[-10^{-3}, 10^3]$  to use a high learning rate in the initial training steps. The size of mini-batch was 10, and the size of patch was  $55 \times 55$  for training. The proposed deep network was implemented using MatConvNet [14] in MATLAB 2015a enviroment (Mathwork, Natick).

## C. Training dataset

We produced the image data from projection data provided by “2016 Low-Dose CT Grand Challenge”. The given raw projection data was obtained by a 2D cylindrical detector and a helical conebeam trajectory using a z-flying focal spot. These have been converted to conventional fanbeam projection data by a single slice rebinning technique. CT images were reconstructed by using a conventional filtered backprojection (FBP) algorithm. The training datasets are composed of routine dose and quarter dose X-ray CT images of 10 patients. The size of the X-ray CT image is  $512 \times 512$  and the slice thickness is 3mm. We used contourlet transform to routine dose X-ray CT images and quarter dose X-ray images. Wavelet coefficients from a quater dose were used for the input  $X'$  and the difference wavelet coefficients between from quarter dose and routine dose image were used for the label  $Y'$ .

## D. Baseline algorithms

For a quantitative evaluation, one patient’s data was used and various image metrics such as peak signal-to-noise ratio (PSNR), structural similarity (SSIM) index, and normalized root mean square error (NRMSE) values were calculated. The test images were denoised by the proposed method and other algorithms such as total variation-based MBIR and the previous CNN in the ‘2016 Low-Dose CT Grand Challenge [6], which we call the AAPM-Net. MBIR regularized by TV was solved by an alternative direction method of multiplier (ADMM) techniques [2] and Chambolle’s proximal TV [15]. The parameter was selected by numerical experiments. Compared to WavResNet in Fig. 1, the AAPM-Net directly learns the countourlet coefficients (with the exception of the lowest frequency residuals) and the other CNN structure is identical. In addition, these two networks were trained with the 9 training datasets of the 10 datasets, and the remaining one data set was used for validation.

## IV. EXPERIMENTAL RESULTS

### A. Improvement over AAPM-Net

First, we presented the denoised images from the dataset of the one patient. This was excluded for the training with routine dose and quarter dose images in Fig. 2(a)(b). The result from AAPM-Net in Fig. 2(c) significantly removes the low-dose noise, but the results appear a bit blurry and lose some details of the texture. On the other hand, the result of WavResNet in in Fig. 2(d) clearly shows the significantly improved noise reduction, while maintaining edges and textures that help to distinguish the lesions in the organ. In the lower part of Fig. 2, the enlarged images are presented and the result of WavResNet clearly identifies the details like the vessels in the liver and some holes. The difference images between denoised images and routine dose image in Fig. 3 confirm the superiority of WavResNet. The difference image of the proposed network contains only the noise of the low-dose X-ray CT image, while the difference image of AAPM-Net contains noise and the edge informations.

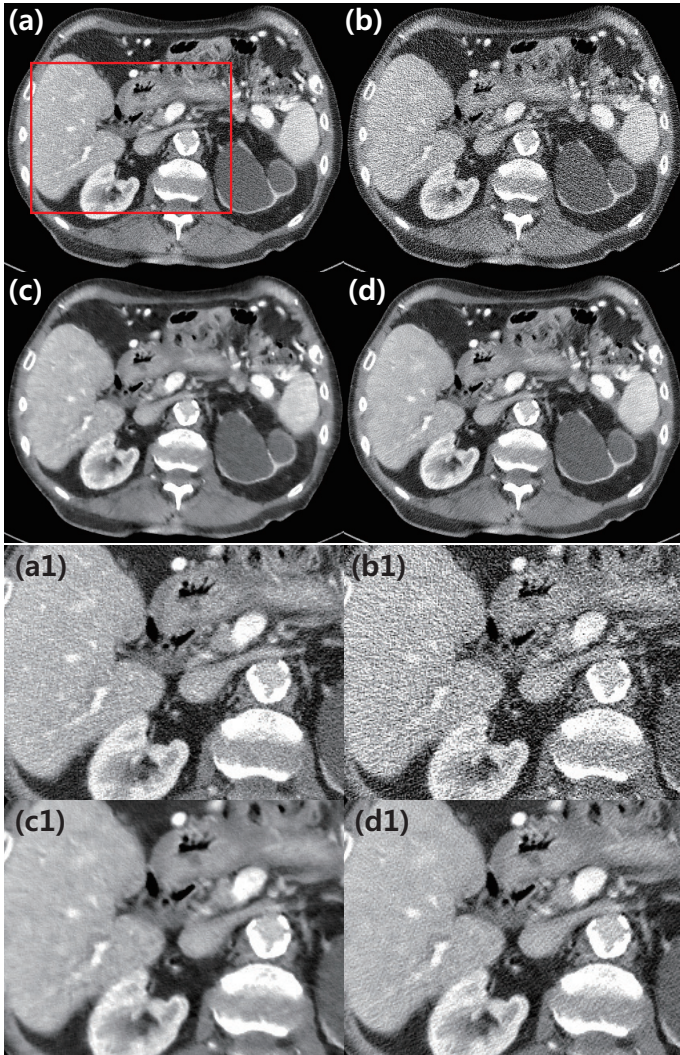


Fig. 2. (a-d) Denoised images with routine dose and quarter dose images. (a1-d1) Magnified images inside the red box. The intensity range was set to (-160, 240) [HU] (Hounsfield Unit). (a,a1) Routine dose, (b,b1) Quarter dose, (c,c1) AAPM-Net, (d,d1) WavResNet.

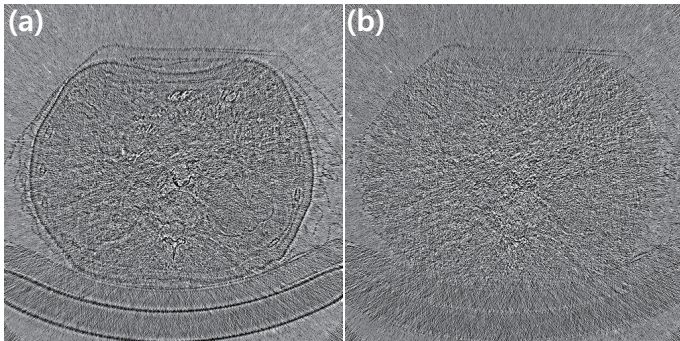


Fig. 3. Difference images between the denoised images and routine dose image. The intensity range was set to (-70,70) [HU]. (a) AAPM-Net, (b) WavResNet.

The convergence plots in Fig. 4 clearly shows the strength of WavResNet. The proposed network exhibits the fast con-

vergence and the final performance surpasses the AAPM-Net with respect to PSNR and NRMSE.

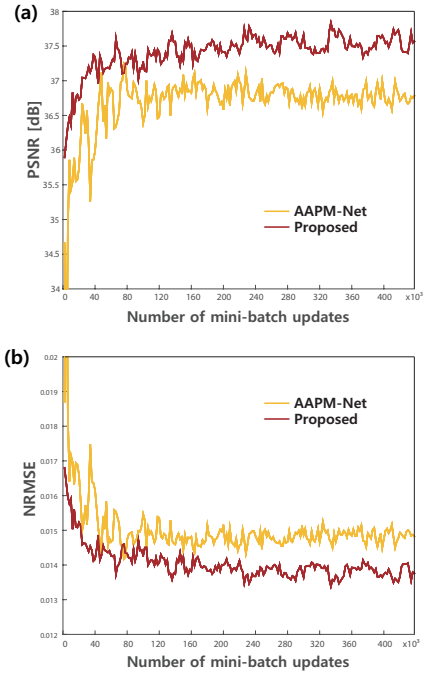


Fig. 4. Convergence plots for (a) PSNR [dB] and (b) NRMSE with respect to each mini-batch updates.

### B. Comparison with existing methods

Since MBIR is currently a standard low-dose reconstruction method, we also compare the results of WavResNet and MBIR. Fig. 5 and Fig. 6 shows examples of comparative experiments. The reconstruction results by MBIR appear a little blurred and the textures are reconstructed incorrectly. On the other hand, WaveResNet provides clear reconstruction results.

Table I presents the averaged PSNR, NRMSE, and SSIM index values of the denoised images from 149 slices. The proposed method showed the highest PSNR and SSIM index value and has the lowest NRMSE value.

|            | MBIR TV | AAPM-Net | Proposed     |
|------------|---------|----------|--------------|
| PSNR [dB]  | 35.34   | 35.85    | <b>36.43</b> |
| NRMSE      | 0.017   | 0.016    | <b>0.015</b> |
| SSIM index | 0.84    | 0.85     | <b>0.87</b>  |

TABLE I

COMPARISON OF LOW-DOSE X-RAY CT RECONSTRUCTION ALGORITHMS.

## V. CONCLUSION

In this paper, we proposed a wavelet domain residual network for low-dose X-ray CT reconstruction. To improve the performance and retain the detailed textures, a high-dimensional embedding scheme using contourlet and residual transform was proposed. These processes simplify the topological structure of input and label data manifold, and allows fast convergence and improved performance. The performance of

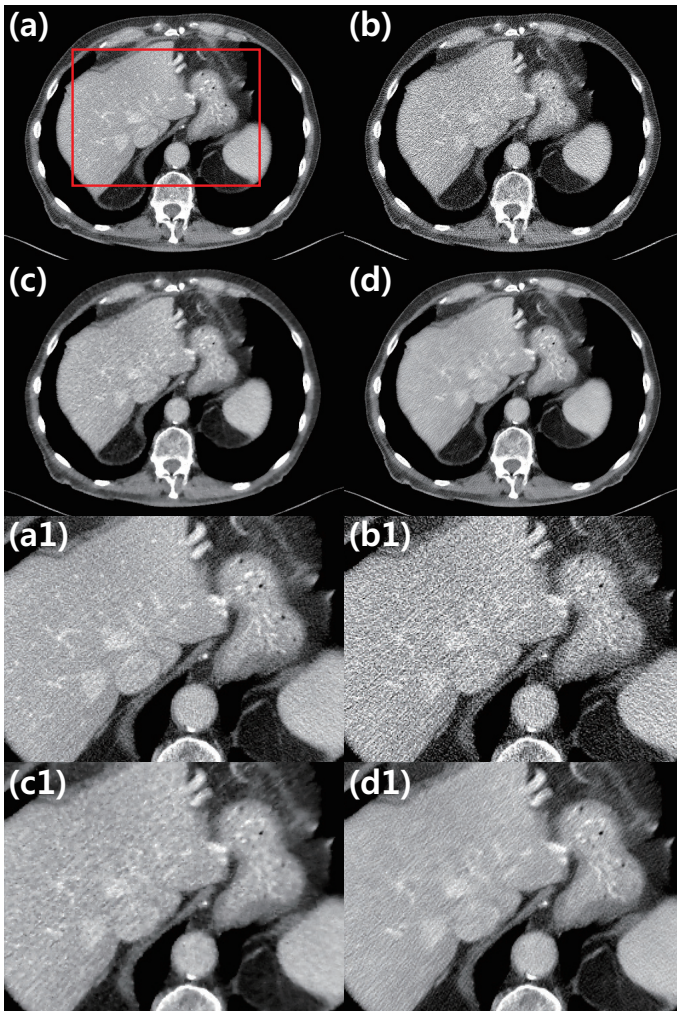


Fig. 5. (a-d) Denoised images with routine dose and quarter dose images. (a1-d1) Magnified images inside the red box. The intensity range was set to (-160, 240) [HU] (Hounsfield Unit). (a,a1) Routine dose, (b,b1) Quarter dose, (c,c1) MBIR TV, (d,d1) WavResNet.

WavResNet has been verified by comprehensive comparative studies against AAPM-Net and MBIR.

#### ACKNOWLEDGMENT

The authors would like to thanks Dr. Cynthia MaCollough, the Mayo Clinic, the American Association of Physicists in Medicine (AAPM), and grant EB01705 and EB01785 from the National Institute of Biomedical Imaging and Bioengineering for providing the Low-Dose CT Grand Challenge data set. This work is supported by Korea Science and Engineering Foundation, Grant number NRF-2016R1A2B3008104.

#### REFERENCES

- [1] M. Beister, D. Kolditz, and W. A. Kalender, "Iterative reconstruction methods in X-ray CT," *Physica medica*, vol. 28, no. 2, pp. 94–108, 2012.
- [2] S. Ramani and J. A. Fessler, "A splitting-based iterative algorithm for accelerated statistical X-ray CT reconstruction," *IEEE transactions on medical imaging*, vol. 31, no. 3, pp. 677–688, 2012.

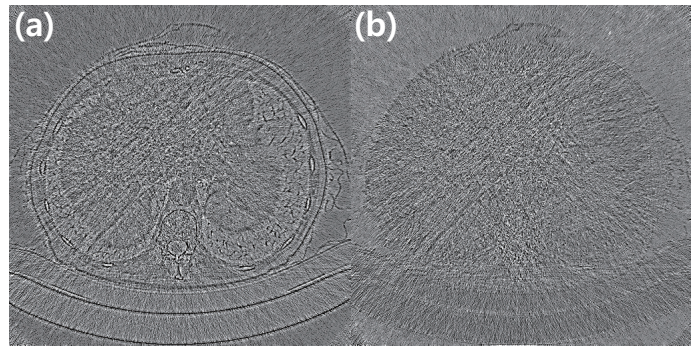


Fig. 6. Difference images between the denoised images and routine dose image. The intensity range was set to (-70,70) [HU]. (a) MBIR TV, (b) WavResNet.

- [3] A. Krizhevsky, I. Sutskever, and G. E. Hinton, "ImageNet classification with deep convolutional neural networks," in *Advances in neural information processing systems*, 2012, pp. 1097–1105.
- [4] Y. Chen, W. Yu, and T. Pock, "On learning optimized reaction diffusion processes for effective image restoration," in *Proceedings of the IEEE Conference on Computer Vision and Pattern Recognition*, 2015, pp. 5261–5269.
- [5] C. Dong, C. C. Loy, K. He, and X. Tang, "Learning a deep convolutional network for image super-resolution," in *European Conference on Computer Vision*. Springer, 2014, pp. 184–199.
- [6] E. Kang, J. Min, and J. C. Ye, "A deep convolutional neural network using directional wavelets for low-dose x-ray ct reconstruction," *arXiv preprint arXiv:1610.09736*, 2016.
- [7] M. Anthony and P. L. Bartlett, *Neural network learning: Theoretical foundations*. Cambridge university press, 2009.
- [8] P. L. Bartlett and S. Mendelson, "Rademacher and gaussian complexities: Risk bounds and structural results," *Journal of Machine Learning Research*, vol. 3, no. Nov, pp. 463–482, 2002.
- [9] M. Telgarsky, "Benefits of depth in neural networks," *arXiv preprint arXiv:1602.04485*, 2016.
- [10] A. J. Smola and B. Schölkopf, *Learning with kernels*. Citeseer, 1998.
- [11] K. Zhang, W. Zuo, Y. Chen, D. Meng, and L. Zhang, "Beyond a gaussian denoiser: Residual learning of deep cnn for image denoising," *arXiv preprint arXiv:1608.03981*, 2016.
- [12] Y. Han, J. Yoo, and J. C. Ye, "Deep residual learning for compressed sensing CT reconstruction via persistent homology analysis," *arXiv preprint arXiv:1611.06391*, 2016.
- [13] J. Zhou, A. L. Cunha, and M. N. Do, "Nonsampled contourlet transform: construction and application in enhancement," in *IEEE International Conference on Image Processing 2005*, vol. 1. IEEE, 2005, pp. I–469.
- [14] A. Vedaldi and K. Lenc, "MatConvNet: Convolutional neural networks for matlab," in *Proceedings of the 23rd ACM international conference on Multimedia*. ACM, 2015, pp. 689–692.
- [15] A. Chambolle, "An algorithm for total variation minimization and applications," *Journal of Mathematical imaging and vision*, vol. 20, no. 1–2, pp. 89–97, 2004.